

Closed-Form Congestion Control via Deep Symbolic Regression

Jean Martins, Igor Almeida, Ricardo Souza, Silvia Lins
Ericsson Research, Indaiatuba, SP – BR

Email: {jean.martins, igor.almeida, ricardo.s.souza, silvia.lins}@ericsson.com

Abstract—As mobile networks embrace the 5G era, the interest in adopting Reinforcement Learning (RL) algorithms to handle challenges in ultra-low-latency and high throughput scenarios increases. Simultaneously, the advent of packetized fronthaul networks imposes demanding requirements that traditional congestion control mechanisms cannot accomplish, highlighting the potential of RL-based congestion control algorithms. Although it is feasible to learn RL policies optimized for satisfying the stringent fronthaul requirements, neural network models’ adoption in real deployments still poses some challenges regarding real-time inference and interpretability. This paper proposes a methodology to deal with such challenges while maintaining the performance and generalization capabilities provided by a baseline RL policy. The method consists of (1) training a congestion control policy specialized in fronthaul-like networks via reinforcement learning, (2) collecting state-action experiences from the baseline, and (3) performing deep symbolic regression on the collected dataset. The proposed process overcomes the challenges related to inference-time limitations through closed-form expressions that approximate the baseline performance (link utilization, delay, and fairness), and which can be directly implemented in any programming language. Finally, we provide an analysis of the closed-form expressions’ inner workings.

Index Terms—Reinforcement learning, symbolic regression, congestion control, real-time inference, model interpretability, fronthaul networks.

I. INTRODUCTION

Emerging 5th Generation Mobile Networks (5G) sparked the interest in more flexible, adaptable, and cost-efficient network architectures. Playing a fundamental role in this context, Centralized Radio Access Networks (C-RAN) [1] offer flexibility and reduced deployment costs, splitting the regular radio base stations into the Baseband Unit (BBU) and the Remote Radio Unit (RRU). With the reduction of RRU node complexity comes the increasing throughput demands imposed on the fronthaul links, 50 times higher than backhaul in some cases [2].

Transitioning from dedicated fiber links (which adopted Common Public Radio Interface (CPRI) [3] protocol) towards packetized network deployments (i.e., with statistical multiplexing) is one strategy to reach more cost-efficient fronthaul solutions. However, shifting to a shared infrastructure introduces additional challenges for the transport network: fronthaul links may experience congestion due to, e.g., aggressive radio schedulers. Traditional congestion control (CC) algorithms often face limitations when dealing with low latency and high throughput demands, leaving the challenge of addressing congestion control in packetized fronthaul networks.

There has been much exploration regarding using machine learning techniques for improvements in TCP CC algorithms, with promising results [4]–[6]. More recently, the interest increased regarding the adoption of deep Reinforcement Learning (RL) algorithms that learn completely new CC policies from scratch [7]–[12].

More specifically, the literature is much less abundant in the scope of packetized fronthaul networks. In this context, RL approaches have the additional challenge of dealing with very high-speed (microsecond) control loops, which impose stringent requirements on the inference time of Neural Network Neural Network (NN) models. If the inference time is slower than the minimum Round Trip Times (RTTs), RL agents cannot be very responsive, which could deteriorate their performance [9]. Another usual concern regarding RL models is their black-box nature. Their low interpretability hides from the practitioner the decision-making process, posing questions on how general the models are, and if they can be broadly trusted.

Overall, those are valid questions, but although RL models usually perform very well in scenarios similar to those observed during the training phase (in training distribution), the open question remains on how to obtain the same guarantee in scenarios unseen during the training phase [13].

This paper proposes a methodology to circumvent all the challenges mentioned earlier. First, to deal with performance issues of general CC, we train a RL baseline policy specialized in fronthaul-like scenarios. Second, to deal with inference-time and interpretability issues, we employ deep symbolic regression to extract closed-form mathematical expressions (symbolic policies) that approximate the RL baseline behavior. The resulting symbolic policies are interpretable and at the same time, easy to implement in any programming language, which completely overcomes any issues with inference time. The results show that such policies also closely follow the overall performance of the RL baseline while matching its generalization capabilities.

The paper is organized as follows. Section II presents symbolic regression, RL, and congestion control background. Section III describes the learning problem, training environment, network simulation technical aspects, and the methodology for learning the symbolic policies. Section IV describes the experiments and results for different network configurations, and Section V presents our concluding remarks.

II. BACKGROUND

A. Reinforcement Learning

RL comprises a set of techniques that enable an agent to learn how to optimally interact with an environment via trial-and-error. The overall goal is to derive policies that map the current observed state $x_t \in \mathcal{X} \subseteq \mathbb{R}^n$ of a system and produce actions $a_t \in \mathcal{A} \subseteq \mathbb{R}$ that maximize the expected cumulative rewards $r : \mathcal{X} \mapsto \mathbb{R}$ received over time [14].

This paper focuses on RL algorithms suitable to environments where the action space is continuous. As a representative example, we describe the Deep Deterministic Policy Gradient (DDPG) [15], which employs an actor-critic architecture combining both Q-learning and policy gradient techniques [14].

The actor is a deterministic policy $\mu_\theta : \mathcal{X} \mapsto \mathcal{A}$ that, given a state, outputs actions in a continuous-space, while the critic is a parameterized Q-value function $Q_\phi : \mathcal{X} \times \mathcal{A} \mapsto \mathbb{R}$ that assess the quality of such actions in terms of expected future rewards. DDPG follows an off-policy strategy which relies on an experience buffer $\mathcal{D} = \{(x_t, a_t, x_{t+1}, r(x_t))\}_{i=0}^\ell$, containing action-induced state transitions [16].

To address DDPG shortcomings regarding the overestimation of Q-values [17], the Twin-Delayed Deep Deterministic Policy Gradient (TD3) algorithm was proposed [18], introducing: (1) clipped double Q-Learning, (2) delayed policy updates (and target networks), and (3) target policy smoothing. TD3 is the baseline RL agent used for the experiments in this paper.

B. Deep symbolic regression

Given a dataset $\mathcal{D} = \{X_i, y_i\}$, where every $X_i \in \mathbb{R}^n$ and labels $y_i \in \mathbb{R}$, symbolic regression is a supervised learning procedure that aims at identifying a function $f : \mathbb{R}^n \mapsto \mathbb{R}$ that minimizes the residual $\|f(X_i) - y_i\|^2$ and whose form is a short mathematical expression defined from a set of predefined tokens. If the dataset \mathcal{D} represents the states observed and the actions taken by an RL policy, then function f is a white-box approximation of such policy. This type of procedures are usually referred to as behavioral cloning of the expert policy [19]. However, depending on the properties of the dataset and the accuracy of the regression process, the expert RL policy and the resulting f may show very different capabilities [20].

In this paper, we employ the deep symbolic regression method proposed by Petersen et al [21]¹. The method employs a neural network controller to represent a distribution over mathematical expressions defined as a sequence of tokens in the pre-order of the corresponding expression tree. As an example, the sequence $\tau = [+ , \sin , x_1 , \exp , x_2]$ corresponds to the expression $f(x) = \sin(x_1) + \exp(x_2)$.

Expressions are sampled autoregressively from the probability distribution learned by the controller, and they are evaluated based on how well they match the dataset $R(\tau, \{X_i, y_i\})$. The controller is then trained to maximize a RL objective based on $\mathbb{E}_\tau = [R(\tau, \{X_i, y_i\})]$. As the training progresses, the controller is able to generate expressions that better match the dataset [22].

¹<https://github.com/brendenpetersen/deep-symbolic-optimization>

III. METHODOLOGY

A. Network simulations

The network environment is a fronthaul simulation developed on Network Simulator 3 (NS-3), with additional support to OpenGym interfaces for RL implemented using ns3-ai [23]. The fronthaul scenario implements a UDP-based constant bitrate communication between pairs of senders (DUs) and their receivers (RUs), which share a bottleneck link in the dumbbell topology of Figure 1. Senders and receivers are connected to switches through individual access links; and these switches exchange packets via the shared communication link. To isolate the dynamics we want to explore, we assume the access links have negligible packet losses and sufficient capacity, so that these impairments are only present in the shared link. To perform the congestion control on top of the UDP-based communication, agents are given control of the intersend time between sent packets, implementing a rate-based congestion control approach.

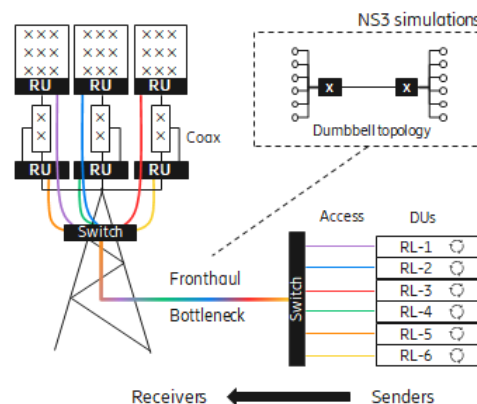


Figure 1: Fronthaul network and its NS3 counterpart.

Typically, congestion control algorithms are event-based, in that they act upon the occurrence of a trigger event, for instance the reception of an ACK or detection of a lost packet from a timeout. The RL agent, on the other hand, was implemented as a time-based algorithm. This allows the agent to observe the impact an action for a while before a new action is taken. Therefore, the observation time window is also a simulation parameter that needs to be defined and influences the overall performance of the agent [9], [24].

B. Learning Problem

The network simulations define a multi-agent scenario where senders must cooperate in order to maximize link utilization and fairness while minimizing the RTTs. Here, we assume a decentralized learning problem where the agents cannot communicate, and only observe their local performance metrics, utilities and rewards. Finally, we also assume that all agents follow the same learned policy.

The observation space is defined by four dimensions $\mathcal{X} \subset \mathbb{R}^4$. At any timestep t , we define x_1^t as the intersend time, x_2^t as the average RTT (observed during the current time window), x_3 as the RTT ratio (x_2 over the minimum observed RTT),

and x_4^t as the packet loss ratio (packet losses over the number of packets sent).

The action space is unidimensional $\mathcal{A} = [0.8, 1.5]$, and the actions $a_t \in \mathcal{A}$ are employed to update the intersend time as follows $x_1^{t+1} := x_1^t/a_t$.

The reward is a linear function of the number of acknowledged packets (acks_t), the average round trip time (RTT_t), and packet losses (losses_t). We assume all measurements are first normalized to the same scale by a function η . Since the reward function is not employed during the evaluation, the normalization function can rely on information that is not accessible after training, e.g., the bounds for number of acknowledged packets (A), RTTs (R), and packet losses (L).

$$r_t = \eta(\text{acks}_t, A) - \eta(\text{RTT}_t, R) - \eta(\text{losses}_t, L) \quad (1)$$

Equation (1) aims at inducing the trained policies to increase the transmission rate until the observed RTTs increase or packet losses occur. Overall, an optimal policy would allow a sender to discover the highest fair transmission rate that maintains the RTTs close to the minimum. The above formulation models congestion control as a decentralized decision-making problem. It is a harsh environment for learning, due to partial observability and the inherent non-stationarity of the network state, but it makes the scenario close to real-world deployments.

C. Deep symbolic regression

Given an expert TD3 policy $\mu_\theta : \mathcal{X} \mapsto \mathcal{A}$, the first step of learning a closed-form congestion control policy is to collect a dataset of experiences from μ_θ in the target environment. Such experiences are then stored as state-action tuples in a dataset $\mathcal{D} = \{(x_i, a_i)\}_{i=1}^N$, where $x_i \in \mathcal{X}$ are observations from the current state and $a_i \in \mathcal{A}$ are the respective actions proposed by the expert policy, $a_i := \mu_\theta(x_i)$.

Such datasets must contain a representative set of experiences. In congestion control tasks, that means samples representing scenarios where the transmission rate should be increased, stabilized, and decreased. To collect samples of such classes, we employ a simple ϵ -greedy exploration strategy, with $\epsilon = 0.5$, in which TD3 actions are chosen half of the time, and random actions chosen otherwise. This simple exploration strategy eventually leads the simulations to states of high RTT values and packet losses.

From a data set \mathcal{D} , and a set of predefined tokens τ , and a maximum length ℓ , a symbolic regression task can be specified whose goal is to learn a closed-form expression capable of approximating the expert decisions (see Figure 2).

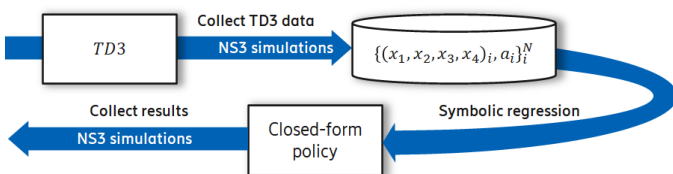


Figure 2: The symbolic regression setup consists of two steps (1) data collection and (2) deep symbolic regression.

The closed-form expressions (or symbolic policies) that result from this process, will achieve different performances depending on their ability to imitate the expert actions in both in-training and out-training distributions.

IV. EXPERIMENTS AND RESULTS

This section compares the learned closed-form congestion control policies to an RL baseline. We assess performance regarding link utilization, packet delay, packet losses, and fairness. We assess generalization capacity by evaluating network scenarios not included in the training datasets.

A. Reinforcement learning baseline

The training environment for the TD3 baseline consists of a set of different network scenarios, defined by their bottleneck capacity and the number of sender-receiver pairs. We employ domain randomization over the bottleneck capacity and the number of sender-receiver pairs [25], according to Table I.

Table I: Network simulation training environment.

Parameter	Domain
Bottleneck capacity	$1Mbps \leq C \leq 2Gbps$
Number of senders	$p \in \{1, 2\}$
Access links	20Gbps (overdimensioned)
Switch queue size	100 packets
Simulation duration	3s
Timestep	1ms

The hyperparameters for the TD3 algorithm followed those employed by [26]. The actor and critic neural networks architectures as $512 \times 16 \times 512$, actor learning-rate 1×10^{-5} , critic learning-rate 5×10^{-5} , multi-step learning with $n = 5$, and $\gamma = 0.999$ (see the reference for more details on this training setup).

B. Closed-form congestion control policies

The symbolic regression method described in III-C produces closed-form expressions that approximate the output label described in the datasets. To stress the generalization capabilities of such policies, we utilize a minimal set of network scenarios for data collection, with a single bottleneck capacity of $C = 500Mbps$.

Following this setup, we collected three different datasets using different numbers of sender-receiver pairs p , here denoted as $\mathcal{D}_{p=1}$, $\mathcal{D}_{p=2}$, and $\mathcal{D}_{p=1,2} = \mathcal{D}_{p=1} \cup \mathcal{D}_{p=2}$. Each dataset contains experiences from 5 seconds NS3 simulations.

Each dataset is input to a deep symbolic regression method, which aims to produce closed-form expressions of maximum length $\ell = 32$ tokens. The set of available tokens is limited to $\tau = \{+, -, \times, \div, \cos\}$. After a fixed amount of time, all runs were stopped, and the best-ranked expression was chosen for the evaluation experiments, which we describe below.

$$\pi_{\mathcal{D}_{p=1,2}} = \cos \left(x_2 + \frac{2x_2}{\frac{x_1}{x_3 + \frac{-x_1+x_2}{x_1}} + x_2} \right) \quad (\text{SP1})$$

$$\pi_{\mathcal{D}_{p=1}} = -\frac{x_3}{x_3 + \frac{\frac{x_1x_3+x_3}{x_2^2}}{x_2x_3}} + \frac{\cos \left(\frac{x_2}{x_1} \right)}{x_3^2} \quad (\text{SP2})$$

$$\pi_{\mathcal{D}_{p=2}} = \cos \left(\frac{x_2x_3(x_2x_3 + x_2 + 2x_3 + x_4)}{x_1 + x_2^2x_3x_4 + x_2x_3^2} \right) \quad (\text{SP3})$$

For reference, x_1, x_2, x_3, x_4 stands for inter-send time, RTT, RTT ratio, and packet loss ratio. It is worth noticing that SP1 and SP2 have ignored the information about packet losses, i.e., x_4 . This is an indication that to approximate the actions in the dataset, such variable was not essential.

Another intriguing characteristic is the presence of tokens such as \cos , whose relevance was identified in preliminary experiments. It introduces a non-linearity that showed benefits in most of the evaluated regression settings.

C. Performance Evaluation

Here we compare the performances of TD3 and the symbolic policies SP1, SP2, and SP3. We design a two-phase set of experiments, where Phase I identifies the most promising symbolic policy in short simulations, and Phase II performs more expensive simulations against the TD3 baseline (Table II).

Table II: Evaluation settings.

Parameter	Phase I (1s)	Phase II (20s)
$C \in$ (Mbps)	250, 500, 1000	250, 500, 1000
$p \in$	{1, 5, 10, 15, 20}	{1, 5, 10, ..., 35, 40}

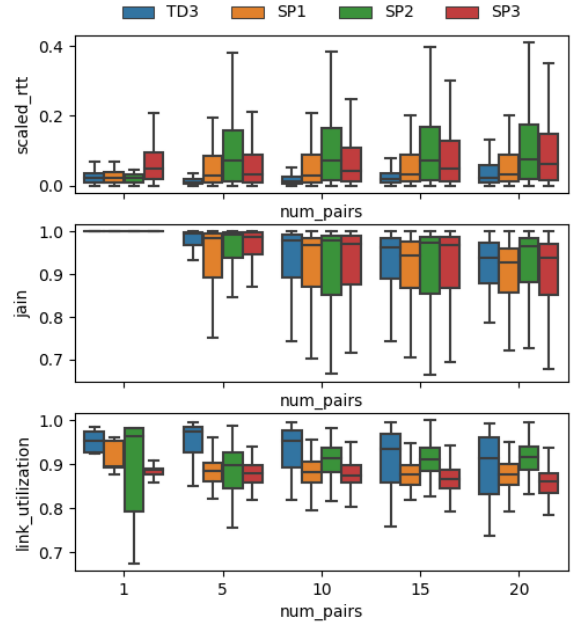
The different bottleneck capacities induce network scenarios with different RTT ranges, while the number of senders impacts the network dynamics. An optimal agent would maintain high link utilization (close to 100% of the bottleneck capacity), average RTTs close to the minimum, and zero packet losses while guaranteeing fair bandwidth shares for each flow. It is also desirable that the trained policies generalize well to a superset of the scenarios seen during training. Therefore, the results here contain simulations with as many as 40 sender-receiver pairs, much more than those observed during training.

To get overall performance picture, we normalized and aggregated all the measurements. Additionally, since there were never packet losses, we only include plots for RTT, Jain fairness index and link utilization.

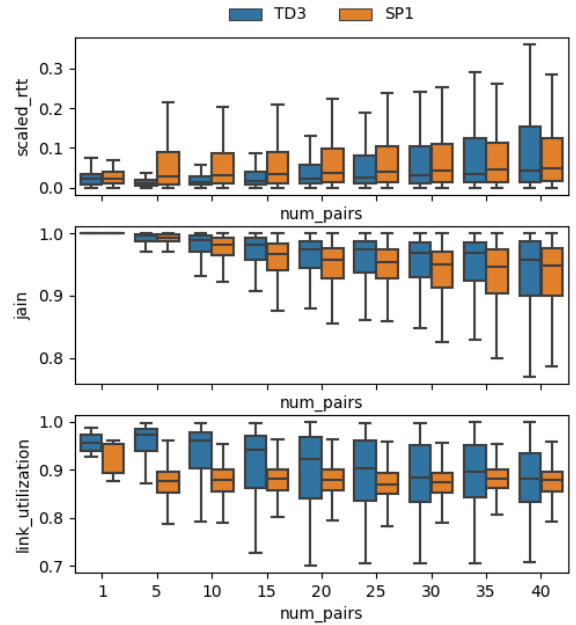
Figure 3a summarizes the results of Phase I. The results illustrate performance in two scenarios, those close to the training distribution and those far from it. In the first scenario, we highlight the case of $p = 1$, that belongs to the training distribution of SP1 and SP2 but not for SP3, where SP3 reached the worst results overall. Conversely, in scenarios with $p \geq 5$ that are out of the training distribution for all symbolic policies, we observe a more stable behavior.

Overall, SP1 and SP3 performed better than SP2 in terms of RTT, which relates to the fact that they are also more

conservative regarding link utilization. We choose SP1 to go for Phase II.



(a) Phase I.



(b) Phase II.

Figure 3: Performance results of Phases I and II.

Figure 3b summarize the Phase II results of SP1 against TD3. Regarding RTT and link utilization, we observe an interesting pattern in which SP1 performance deteriorates slower than TD3 as p increases. This is an impressive result that provides evidence for high generalization capacity of the symbolic policies. Regarding the Jain fairness index, all the policies variances increased very similarly with p . Regarding

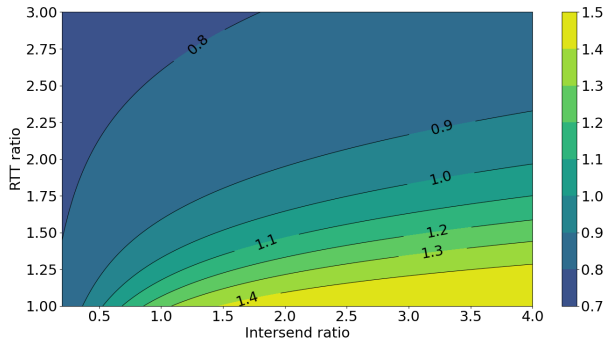


Figure 4: Contours of simplified SP1 for $C = 1000\text{Mbps}$.

link utilization, we again see a slower deterioration of SP1 performance when compared to TD3.

D. Analysis and visualization

We turn now to a brief investigation on the symbolic policy’s ability to cope with different scenarios and network conditions. Due to space constraints, we focus only on SP1 and a few examples that illustrate our main points. Furthermore, we work around the challenges introduced by a four-dimensional observation space with convenient slices, as will be explained in the next paragraphs.

In line with previous work on visualizing such models [26], Figure 4 presents contours of the output of SP1, remapped to action space \mathcal{A} . The axes are “Intersend ratio” and “RTT ratio”. Indeed, it is possible to rewrite SP1 in terms of a minimum RTT c (primarily defined by link speeds in the topology):

$$f(i_{\text{ratio}}, \text{rtt}_{\text{ratio}}) = n(\pi_{\mathcal{D}_{p=1,2}}(i_{\text{ratio}} \cdot c, \text{rtt}_{\text{ratio}} \cdot c, \text{rtt}_{\text{ratio}})), \quad (2)$$

where $x_1 = i_{\text{ratio}} \cdot c$ is the observed packet intersend time and $x_2 = \text{rtt}_{\text{ratio}} \cdot c$ is the observed RTT, in terms of $x_3 = \text{rtt}_{\text{ratio}}$, and $n(\cdot)$ simply converts the $[-1, 1]$ range to \mathcal{A} .

With Eq. (2), we can interpret the horizontal axis of Figure 4 as the agent’s *offered load* – normalized to the minimum RTT of the network –, where a value of 0.5 would signify sending 2 packets of data per round-trip time, and a value of 4.0 would denote a much less “aggressive” sender that issues a single packet of data every four round-trip times. This can be easily translated to a bit-rate, e.g. in Mbps, if the data packets are of the same size. In the vertical axis, one can explore several *network conditions* via the observed RTT ratio, with a value of 1.0 signifying empty queues in the forward and reverse paths and a value of 2.0 denoting double the minimum RTT.

We draw attention to the 1.0 contour line in Figure 4, which indicates that the offered load should not be changed. Above that, the darker regions on higher RTT ratio values have outputs that *increase* the intersend time, lowering the offered load; whereas the brighter yellow regions on higher intersend ratios indicate that agents with presumably small offered loads can increase them more dramatically than agents whose packets leave more frequently. We note that the heatmap for a scenario with a 100-Mbps bottleneck is very similar, indicating that this “fairness” behavior is also present on more capacity-limited scenarios, though we elide that figure due to space constraints.

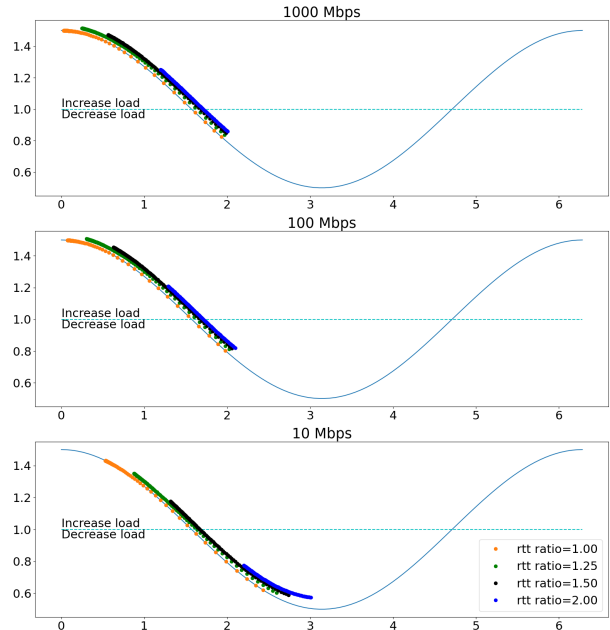


Figure 5: Span of SP1 policy values over the cosine domain.

It is not immediately clear what benefits the introduction of a cosine function brings to the policy’s performance. With this in mind, we investigate SP1’s output with respect to several intersend ratio values, with slices across different RTT ratios and bottleneck link speeds (as defined by a minimum RTT).

This is depicted in Figure 5, where the simplified SP1 is plotted against the $[0, 2\pi]$ domain of the cosine function. In this figure, the intersend ratio varies in the $[0.2, 10.0]$ range, and we artificially separate the dots from each slice vertically, for ease of understanding. One can see that, for the $\text{rtt}_{\text{ratio}} = 1.0$ slice, i.e. no queueing in the network, most of the actions are in the “Increase load” region though, understandably, this behavior becomes less prominent as the bottleneck link capacity gets smaller. In general, this figure illustrates that the policy adapts its output for different scenarios and conditions by evaluating different regions of its underlying non-linear functions.

As an extension of Figure 5, we plot below the new intersend ratio values an agent would employ after evaluating the SP1 policy – unlike the previous figures, the no-change region in Figure 6 is the dashed $x = y$ line. Once more, we draw attention to the similarity in the outputs for scenarios with very different capacities, and the general trend of avoiding excessive load in extremely limited scenarios.

V. CONCLUSIONS

Recent results have shown that specialized Reinforcement Learning (RL) congestion control policies are effective alternatives in cases where traditional algorithms do not perform well. However, the deployment of NN models comes with challenges regarding performance, inference time, and generalization guarantees. In the context of ultra-low-latency packetized fronthaul networks, for example, a low inference time is a hard requirement that might restrict the applicability of certain policies in the real world.

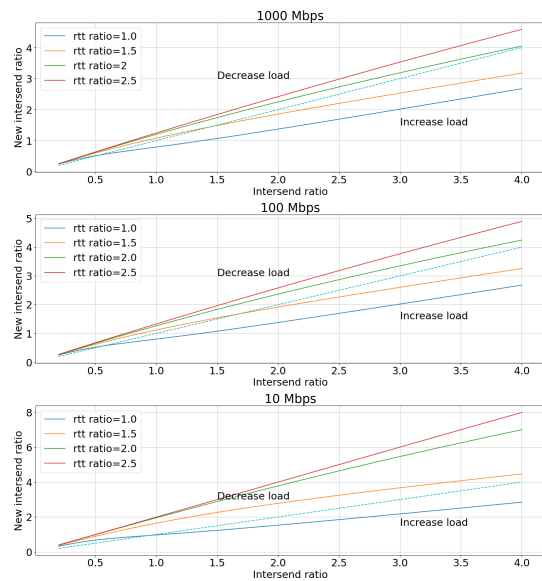


Figure 6: New intersend ratio for several bottleneck scenarios.

This paper proposed and evaluated the use of deep symbolic regression for overcoming inference time challenges while enabling model interpretability and maintaining reasonable generalization capabilities. We trained a fronthaul-specific congestion control policy via RL, and then employed deep symbolic regression on small state-action datasets collected from the RL baseline experiences. This process produced closed-form symbolic policies whose output approximates the actions output by TD3.

The results confirmed that the resulting closed-form policies could maintain a performance very similar to that of RL baseline both in- and out-distribution of training data, which means significant generalization capabilities. Additionally they resolve any eventual issue with inference time since they can be directly implemented in any programming language.

REFERENCES

- [1] M. Jaber, M. A. Imran, R. Tafazolli, and A. Tukmanov, "5g backhaul challenges and emerging research directions: A survey," *IEEE Access*, vol. 4, pp. 1743–1766, 2016.
- [2] H. Holma and A. Toskala, *LTE advanced: 3GPP Solution for IMT-Advanced*. John Wiley & Sons, 2012.
- [3] D. Chitimala, K. Kondepu, L. Valcarenghi, M. Tornatore, and B. Mukherjee, "5g fronthaul-latency and jitter studies of cpri over ethernet," *Journal of Optical Communications and Networking*, vol. 9, no. 2, pp. 172–182, 2017.
- [4] N. Jay, N. Rotman, B. Godfrey, M. Schapira, and A. Tamar, "A deep reinforcement learning perspective on internet congestion control," in *International Conference on Machine Learning*. PMLR, 2019, pp. 3050–3059.
- [5] T. Zhang and S. Mao, "Machine learning for end-to-end congestion control," *IEEE Communications Magazine*, vol. 58, no. 6, pp. 52–57, 2020.
- [6] W. Wei, H. Gu, and B. Li, "Congestion control: A renaissance with machine learning," *IEEE Network*, pp. 1–8, 2021.
- [7] K. Xiao, S. Mao, and J. K. Tugnait, "Tcp-drinc: Smart congestion control based on deep reinforcement learning," *IEEE Access*, vol. 7, pp. 11 892–11 904, 2019.
- [8] L. Liu and H. Xu, "Tyrus: Phy-assisted neural adaptive congestion control for cellular networks," in *Proceedings of the ACM SIGCOMM 2019 Conference Posters and Demos*, ser. SIGCOMM Posters and Demos '19. New York, NY, USA: Association for Computing Machinery, 2019, p. 45–47. [Online]. Available: <https://doi.org/10.1145/3342280.3342302>

- [9] S. Abbasloo, C.-Y. Yen, and H. J. Chao, "Classic meets modern: A pragmatic learning-based congestion control for the internet," in *Proceedings of the Annual Conference of the ACM Special Interest Group on Data Communication on the Applications, Technologies, Architectures, and Protocols for Computer Communication*, ser. SIGCOMM '20. New York, NY, USA: Association for Computing Machinery, 2020, p. 632–647. [Online]. Available: <https://doi.org/10.1145/3387514.3405892>
- [10] S. Emará, B. Li, and Y. Chen, "Eagle: Refining congestion control by learning from the experts," in *IEEE INFOCOM 2020 - IEEE Conference on Computer Communications*, 2020, pp. 676–685.
- [11] W. Li, F. Zhou, K. R. Chowdhury, and W. Meleis, "Qtcp: Adaptive congestion control with reinforcement learning," *IEEE Transactions on Network Science and Engineering*, vol. 6, no. 3, pp. 445–458, 2019.
- [12] I. Nascimento, R. Souza, S. Lins, A. Silva, and A. Klautau, "Deep reinforcement learning applied to congestion control in fronthaul networks," in *2019 IEEE Latin-American Conference on Communications (LATINCOM)*, 2019, pp. 1–6.
- [13] R. Kirk, A. Zhang, E. Grefenstette, and T. Rocktäschel, "A survey of generalisation in deep reinforcement learning," *CoRR*, vol. abs/2111.09794, 2021. [Online]. Available: <https://arxiv.org/abs/2111.09794>
- [14] R. S. Sutton and A. G. Barto, *Introduction to reinforcement learning*. MIT press Cambridge, 1998, vol. 135.
- [15] T. P. Lillicrap, J. J. Hunt, A. Pritzel, N. Heess, T. Erez, Y. Tassa, D. Silver, and D. Wierstra, "Continuous control with deep reinforcement learning," in *4th International Conference on Learning Representations, ICLR 2016, San Juan, Puerto Rico, May 2-4, 2016, Conference Track Proceedings*, Y. Bengio and Y. LeCun, Eds., 2016. [Online]. Available: <http://arxiv.org/abs/1509.02971>
- [16] V. Mnih, K. Kavukcuoglu, D. Silver, A. A. Rusu, J. Veness, M. G. Bellemare, A. Graves, M. Riedmiller, A. K. Fidjeland, G. Ostrovski et al., "Human-level control through deep reinforcement learning," *Nature*, vol. 518, no. 7540, p. 529, 2015.
- [17] H. v. Hasselt, A. Guez, and D. Silver, "Deep reinforcement learning with double q-learning," in *Proceedings of the Thirtieth AAAI Conference on Artificial Intelligence*, ser. AAAI'16. AAAI Press, 2016, pp. 2094–2100.
- [18] S. Fujimoto, H. van Hoof, and D. Meger, "Addressing function approximation error in actor-critic methods," in *Proceedings of the 35th International Conference on Machine Learning*, ser. Proceedings of Machine Learning Research, J. Dy and A. Krause, Eds., vol. 80. PMLR, 10–15 Jul 2018, pp. 1587–1596. [Online]. Available: <https://proceedings.mlr.press/v80/fujimoto18a.html>
- [19] A. O. Ly and M. Akhlofi, "Learning to drive by imitation: An overview of deep behavior cloning methods," *IEEE Transactions on Intelligent Vehicles*, vol. 6, no. 2, pp. 195–209, 2021.
- [20] S.-M. Udrescu and M. Tegmark, "Ai feynman: A physics-inspired method for symbolic regression," *Science Advances*, vol. 6, no. 16, p. eaay2631, 2020.
- [21] B. K. Petersen, M. L. Larma, T. N. Mundhenk, C. P. Santiago, S. K. Kim, and J. T. Kim, "Deep symbolic regression: Recovering mathematical expressions from data via risk-seeking policy gradients," in *International Conference on Learning Representations*, 2021. [Online]. Available: <https://openreview.net/forum?id=m5Qsh0kBBQG>
- [22] M. Landajuela, C. Lee, J. Yang, R. Glatt, C. P. Santiago, I. Aravena, T. N. Mundhenk, G. Mulcahy, and B. K. Petersen, "A unified framework for deep symbolic regression," in *Advances in Neural Information Processing Systems*, A. H. Oh, A. Agarwal, D. Belgrave, and K. Cho, Eds., 2022. [Online]. Available: <https://openreview.net/forum?id=2FNnBhwJsHK>
- [23] H. Yin, P. Liu, K. Liu, L. Cao, L. Zhang, Y. Gao, and X. Hei, "Ns3-ai: Fostering artificial intelligence algorithms for networking research," in *Proceedings of the 2020 Workshop on Ns-3*, ser. WNS3 2020. New York, NY, USA: Association for Computing Machinery, 2020, p. 57–64. [Online]. Available: <https://doi.org/10.1145/3389400.3389404>
- [24] L. Zhang, K. Zhu, J. Pan, H. Shi, Y. Jiang, and Y. Cui, "Reinforcement learning based congestion control in a real environment," in *2020 29th International Conference on Computer Communications and Networks (ICCCN)*. IEEE, 2020, pp. 1–9.
- [25] J. Tobin, R. Fong, A. Ray, J. Schneider, W. Zaremba, and P. Abbeel, "Domain randomization for transferring deep neural networks from simulation to the real world," in *2017 IEEE/RSJ International Conference on Intelligent Robots and Systems (IROS)*, 2017, pp. 23–30.
- [26] J. P. Martins, I. Almeida, R. Souza, and S. Lins, "Policy distillation for real-time inference in fronthaul congestion control," *IEEE Access*, vol. 9, pp. 154 471–154 483, 2021.